Production of e^+ e^- pairs in proton-deuteron capture to ^{3}He

A. Yu. Korchin *, D. Van Neck and M. Waroquier
Department of Subatomic and Radiation Physics, University of Gent, B-9000 Gent, Belgium

O. Scholten and A. E. L. Dieperink
Kernfysisch Versneller Instituut, 9747 AA Groningen, The Netherlands

Abstract

The process $p + d \leftrightarrow {}^3\mathrm{He} + \gamma^*$ at intermediate energies is described using a covariant and gauge-invariant model, and a realistic pd^{3}He vertex. Both photodisintegration of ^{3}He and proton-deuteron capture with production of e^+e^- pairs are studied, and results for cross sections and response functions are presented. The effect of time-like form factors on the dilepton cross sections is investigated as well.

PACS: 21.45.+v, 25.40.Lw, 25.20.Lj
Key Words: dilepton production; proton-deuteron radiative capture; response functions; photodisintegration of ^{3}He

---

*Permanent address: National Science Center 'Kharkov Institute of Physics and Technology', 310108 Kharkov, Ukraine

I. INTRODUCTION

The electromagnetic probe is a well-established and powerful tool to investigate the structure of hadronic systems. In exclusive processes one can distinguish three different regimes depending on the four-momentum of the photon. First, in the space-like region ($q^2 < 0$) in quasi-free kinematics the $(e, e'p)$ reaction directly probes the single-particle structure of the nuclear vertex. Second, for real photons, the (γ, p) or (p, γ) reactions are more sensitive to the details of the reaction mechanism and to meson exchange currents (MEC). Third, the rather less well-known time-like region ($q^2 > 0$), which can be explored using dilepton production, addresses additional aspects as compared to real photons: (i) the coupling of longitudinally polarized photons, (ii) the time-like form factor in the "unphysical" region ($4m_e^2 < q^2 < 4m_p^2$). Basically there are two alternatives to explore the time-like region: virtual Compton scattering $p(\gamma, \gamma^*)p$ and the bremsstrahlung processes with virtual photons, such as $p + p \to p + p + \gamma^*$ and capture reactions.

In this paper we study the capture reaction $p + d \to {}^3\mathrm{He} + \gamma^*$ at intermediate energies (proton energies up to a few hundred MeV) for both real and virtual photons. The main motivation for the present work are experiments at TSL (Uppsala) which in the past have explored [1] only small photon invariant masses ($q^2 <$(10 MeV)^2) and KVI (Groningen) experiments which cover larger photon invariant masses [2].

Since we feel it is important to satisfy gauge invariance, we start from the covariant impulse appoximation model of [3] and make it explicitly gauge invariant by the introduction of an additional internal amplitude. An important input in this approach is the pd^{3}He vertex function, for which recent calculations [4–6] using a realistic NN interaction (Argonne v14 and v18) are used.

II. DESCRIPTION OF THE MODEL

At small photon energies the photon production amplitude is dominated by radiation from the external legs (first three diagrams of Fig. 1), and this consideration led to the development of low-energy theorems (LET)s [7–9]. In kinematical conditions where the photon energy is not small we may still assume the dominance of the above external amplitude, without applying an expansion in powers of the photon energy.

The 4-momenta of the proton, deuteron, ^{3}He nucleus, and (virtual) photon are denoted by p_1, p_2, p_3, and q respectively. The external invariant amplitude reads as

$$M_{ext} = e\,\epsilon_\mu^*(\lambda_\gamma)\,\bar{u}(\vec{p}_3, \lambda_h)\,M_{ext}^{\mu\alpha}\,u(\vec{p}_1, \lambda_p)\,\xi_\alpha(\lambda_d)\,, \tag{1}$$

with

$$\begin{aligned} M_{ext}^{\mu\alpha} = {} & \Phi^\alpha(p_3, p_2, p_1 - q) S(p_1 - q, m_1) \Gamma^\mu(p_1 - q, p_1) \\ & + \Phi^\beta(p_3, p_2 - q, p_1) \Delta_{\beta\rho}(p_2 - q) \Gamma^{\rho\alpha\mu}(p_2 - q, p_2) \\ & + \Gamma^\mu(p_3, p_3 + q) S(p_3 + q, m_3) \Phi^\alpha(p_3 + q, p_2, p_1)\,, \end{aligned} \tag{2}$$

where $\epsilon_\mu^*(\lambda_\gamma)$ and $\xi_\alpha(\lambda_d)$ are the polarization vectors of the photon and the deuteron respectively, $\bar{u}(\vec{p}_3, \lambda_h)$ ($u(\vec{p}_1, \lambda_p)$) is the spinor for ^{3}He (proton) , e is the proton charge, $S(k, m)$

is the free propagator of the fermion with mass m, $\Delta_{\beta\rho}(k)$ is the deuteron propagator. Helicities of the particles are denoted by λ's. The structure of the pd$\rightarrow^3$He vertex function Φ^α will be discussed later.

We stress here that in this formulation the s-amplitude (third diagram in Fig. 1) takes into account the pole contribution (but not the regular contribution) of the initial state pd interaction, and hence takes care of the problem with the orthogonality between initial and final state, mentioned in [10].

The electromagnetic (em) vertex function for spin-$\frac{1}{2}$ particles is chosen in the form

$$\Gamma^\mu(p-q,\,p) = \Gamma^\mu(p,\,p+q) = Z\gamma^\mu - i\frac{\sigma^{\mu\nu}q_\nu}{2m}F_2(q^2) + Z\tilde{F}_1(q^2)(q^\mu \not{q} - q^2\gamma^\mu)\,, \tag{3}$$

where $F_1(q^2)$ and $F_2(q^2)$ are respectively the Dirac and Pauli em form factor (FF), $\tilde{F}_1(q^2) \equiv [1-F_1(q^2)]/q^2$, and $Z = 1\,(2)$ for the proton (^{3}He). This vertex obeys the Ward-Takahashi identity for the half-off-shell case [11].

The half-off-shell γdd vertex satisfying the corresponding Ward-Takahashi identity [8] can be written as

$$\Gamma^{\rho\alpha\mu}(p_2-q,p_2) = -g^{\rho\alpha}(2p_2-q)^\mu + (p_2-q)^\rho g^{\mu\alpha} + \tilde{F}_1(q^2)g^{\rho\alpha}[q^2(2p_2-q)^\mu - q\cdot(2p_2-q)q^\mu]$$
$$+F_2(q^2)(q^\rho g^{\mu\alpha} - q^\alpha g^{\mu\rho}) + \frac{F_3(q^2)}{2m_2^2}[\,q^\rho q^\alpha(2p_2-q)^\mu - \frac{1}{2}q\cdot(2p_2-q)(q^\alpha g^{\mu\rho} + q^\rho g^{\mu\alpha})\,]\,, \tag{4}$$

where $F_i(q^2)$ are related to the charge $G_C(q^2)$, magnetic $G_M(q^2)$, and quadrupole $G_Q(q^2)$ em FFs of the deuteron (see, e.g., [12]).

Apart from the amplitude M_{ext} corresponding to radiation from the external legs there are other more complicated processes, such as initial-state pd rescattering and MEC. This contribution (henceforth called the internal amplitude M_{int}) can be constrained by imposing the gauge invariance requirement for the total amplitude $M = M_{ext}+M_{int}$. Such a procedure is conventionally applied in derivations of the LET for bremsstrahlung [7]. We will make use of consequences of gauge invariance in situations where the photon energy is not small.

One can show that the internal amplitude obeys the following condition

$$q_\mu M_{int}^{\mu\alpha} = -q_\mu M_{ext}^{\mu\alpha} = \Phi^\alpha(p_3,p_2,p_1-q) + \Phi^\alpha(p_3,p_2-q,p_1) - 2\Phi^\alpha(p_3+q,p_2,p_1)\,. \tag{5}$$

The pd^{3}He vertex function for the case where at most one particle is off its mass shell has the following structure [3]

$$\Phi^\alpha(k_3,k_2,k_1) = \phi_+^\alpha(k_3,k_2,k_1) + \phi_-^\alpha(k_3,k_2,k_1)\frac{\not{k}_1 - m_1}{2m_1} + \frac{\not{k}_3 - m_3}{2m_3}\phi_-^\alpha(k_3,k_2,k_1)\,, \tag{6}$$

where the last two terms correspond to negative energy states and only contribute when the proton or the helion are off their mass shells. We will use a form for the $\phi_\pm^\alpha$ which allows a direct relation with the nonrelativistic wave function (WF)

$$\phi_\pm^\alpha(k_3,k_2,k_1) = [\,\gamma^\alpha G_\pm(Q^2) - Q^\alpha H_\pm(Q^2)\,]\gamma_5\,, \tag{7}$$

where $Q^\alpha = \frac{M_r}{m_1}k_1^\alpha - \frac{M_r}{m_2}k_2^\alpha$ is the relative pd 4-momentum and $M_r = m_1m_2/(m_1+m_2)$ is the reduced mass of the pd system. For the ^{3}He, proton and deuteron diagram in Fig. 1 the

relative momenta take the values $Q_3^\alpha = \frac{M_r}{m_1}p_1^\alpha - \frac{M_r}{m_2}p_2^\alpha$, $Q_1^\alpha = Q_3^\alpha - \frac{M_r}{m_1}q^\alpha$ and $Q_2^\alpha = Q_3^\alpha + \frac{M_r}{m_2}q^\alpha$ respectively.

From Eqs. (5-7) it follows that a solution for the internal amplitude can be constructed as $M_{int}^{\mu\alpha} = M_{int}^{\mu\alpha}(1) + M_{int}^{\mu\alpha}(2)$, where

$$M_{int}^{\mu\alpha}(1) = \{\,[\gamma^\alpha G_-(Q_1^2) - Q_1^\alpha H_-(Q_1^2)]\frac{\gamma^\mu}{2m_1} - \frac{\gamma^\mu}{m_3}[\gamma^\alpha G_-(Q_3^2) - Q_3^\alpha H_-(Q_3^2)]\,\}\gamma_5$$
$$+g^{\mu\alpha}\,[\,\frac{M_r}{m_1}H_+(Q_1^2) - \frac{M_r}{m_2}H_+(Q_2^2)\,]\gamma_5\,, \qquad (8)$$

$$M_{int}^{\mu\alpha}(2) = \frac{M_r}{m_1}(q-2p_1)^\mu R_1^\alpha + \frac{M_r}{m_2}(q-2p_2)^\mu R_2^\alpha + \frac{M_r}{m_1+m_2}(q+2p_3)^\mu(R_1^\alpha + R_2^\alpha)\,. \qquad (9)$$

We have used the notations (for i=1,2)

$$R_i^\alpha = [\gamma^\alpha G'_+(Q_i^2) - Q_3^\alpha H'_+(Q_i^2)]\gamma_5\ , \qquad G'_+(Q_i^2) = \frac{G_+(Q_i^2) - G_+(Q_3^2)}{Q_i^2 - Q_3^2} \qquad (10)$$

and similar notations for $H'_+(Q_i^2)$. Note, that this amplitude remains finite in the special cases where $Q_1^2 \to Q_3^2$ or $Q_2^2 \to Q_3^2$. As a check of our results we verified that $M = M_{ext} + M_{int}$ reproduces the LET amplitude of [9] for real photons when $q \to 0$.

We include in the calculation the dominant components [4,6] of the ^{3}He WF, i.e. a pn pair in the deuteron state or in the $^1S_0$ (quasi) bound d^* state, coupled to a proton. We neglect contributions to the amplitude where the deuteron is excited into the $T = 0$ continuum. The $pd \to pd^*$ capture mechanism via the spin-flip $^3S_1 +^3 D_1 \to^1 S_0$ transition has been shown [3] to be important and is therefore included explicitly in M_{ext}. The corresponding amplitude (Fig. 1, last graph) can be written as

$$M_{d*}^{\mu\alpha} = \Psi(p_3, p_2 - q, p_1)\Delta(p_2 - q)\Gamma^{\mu\alpha}(p_2 - q, p_2)\,, \qquad (11)$$

where $\Delta(k) = (k^2 - m_2^{*2} + i0)^{-1}$ and the em vertex has the form

$$\Gamma^{\mu\alpha}(p_2 - q, p_2) = -\frac{i}{m_1}\mu_v \varepsilon^{\mu\alpha\rho\nu} q_\rho (p_2)_\nu F(q^2)\,. \qquad (12)$$

Here $\mu_v = \mu_p - \mu_n$ is the isovector magnetic moment of the nucleon, m_2^* is the mass of the d^*, $F(q^2)$ is the transition FF and $\Psi(p_3, p_2 - q, p_1)$ is the pd*^{3}He vertex function. This contribution is gauge invariant and does not affect the above discussion of the gauge invariance.

The invariant functions $G_\pm(Q^2)\,, H_\pm(Q^2)$ can be related to the S and D components of the overlap integral $< d\,|\,^3He >$. For this purpose the formalism developed previously in [13] for the pnd vertex and also in [3] has been applied. In the same way the vertex $\Psi(p_3, p_2 - q, p_1)$ has been expressed through the overlap integral $< d^*\,|\,^3He >$. Two models for the ^{3}He WF have been used in calculations. The first one is the parametrization in [3] of the calculations in Ref. [4] with the Argonne v14 NN + Urbana VII 3N interaction. The second model is a more recent calculation [6] with the Argonne v18 NN + Urbana IX 3N interaction.

In order to calculate the em FFs of the proton we used the extended vector meson dominance model [14]. The deuteron FFs at negative q^2 are taken from the calculation in

[5], and we used the parametrization of the FFs of the ^{3}He as given in [15]. The proton FFs are continuous functions when going from negative to positive q^2, and this behaviour is incorporated in the VMD models. For the deuteron and the helion we have made the assumption that the em FFs have a smooth extrapolation from the space-like to the time-like region. In this paper we are interested in the interval of relatively small photon invariant masses, restricted by the proton incoming energy T_p of about 300 MeV. Since the maximal photon invariant mass $m_\gamma^{max} = \sqrt{s} - m_3 \approx 2/3\, T_p\,,$ q^2 does not exceed 0.04 GeV^2 and the above approximation should give a reasonable estimate of the effect of FFs on the dilepton cross sections. Finally, the FF of the transition $d \to d^*$ at positive q^2 is chosen the same as the deuteron FF $F_1(q^2)$.

At the real photon point the FFs are normalized to

$$F_1^p(0) = F_1^h(0) = G_C(0) = 1\,, \qquad F_2^p(0) = \mu_p - 1\,, \qquad F_2^h(0) = \frac{m_3}{m_1}\mu_h - 2\,,$$
$$G_M(0) = \frac{m_2}{m_1}\mu_d\,, \qquad G_Q(0) = m_2^2 Q_d\,, \tag{13}$$

where $Q_d = 0.2859$ fm^2 is the quadrupole moment of the deuteron and the magnetic moments of the proton, deuteron, and ^{3}He (in nuclear magnetons) are $\mu_p = 2.7928$, $\mu_d = 0.85774$, and $\mu_h = -2.12755$ respectively.

III. CROSS SECTION AND RESPONSE FUNCTIONS FOR DILEPTON PRODUCTION

The c.m. cross section for the p+d $\to$ ^{3}He+$e^+ + e^-$ reaction can be decomposed (in complete analogy to the spacelike $(e, e'p)$ reaction) into the sum of products of kinematical factors and four response functions (RFs),

$$\frac{d\,\sigma\,(e^+e^-)}{d\,\Omega_\gamma d\,m_\gamma d\,\Omega_e^*} = \frac{\alpha^2 m_1 m_3 q_c \beta}{16\pi^3 m_\gamma p_c s}\,[\,W_T\,(1 - \frac{1}{2}\beta^2\sin^2\theta^*) + W_L\,(1 - \beta^2\cos^2\theta^*)$$
$$+ W_{TT}\,\frac{1}{2}\beta^2\sin^2\theta^*\cos 2\phi^* + W_{LT}\,\frac{1}{2\sqrt{2}}\beta^2\sin 2\theta^*\cos\phi^*\,]\,. \tag{14}$$

Here $m_\gamma = \sqrt{q^2}$ is the invariant mass of the virtual photon, $s = (m_1 + m_2)^2 + 2m_2 T_p\,,$ T_p is the proton kinetic energy in the lab frame, p_c and q_c are the c.m. 3-momenta of the proton (deuteron) and photon (helion) respectively, $\alpha = 1/137.035$, $\beta = (1 - 4m_e^2/m_\gamma^2)^{1/2}$ and m_e is the electron mass. For a description of the kinematics and details about the decomposition of the e^+e^- cross section into the independent RFs W_i we refer to [10]. The differential $d\,\Omega_e^*$ in Eq. (14) is written in the photon rest frame (denoted by *) [10], but can easily be transformed back to the proton-deuteron c.m. frame (see [16]).

The RFs in Eq. (14) contain information on the hadronic transition. They depend on three variables ($W_i \equiv W_i(s, m_\gamma, \theta_\gamma)$) and are defined as

$$W_T = \frac{1}{6}\sum_{polar.}(|J_x|^2 + |J_y|^2)\,, \qquad W_L = \frac{1}{6}\frac{m_\gamma^2}{q_0^2}\sum_{polar.}|J_z|^2\,,$$
$$W_{TT} = \frac{1}{6}\sum_{polar.}(|J_y|^2 - |J_x|^2)\,, \qquad W_{LT} = -\frac{1}{6}\frac{m_\gamma}{q_0}\sum_{polar.} 2\sqrt{2}\,\Re\,(J_z J_x^*)\,, \tag{15}$$

where $q_0 = (m_\gamma^2 + \vec{q}_c^{\,2})^{1/2}$ is the energy of the virtual photon, and the space components of the em current $J^\mu \equiv \bar{u}(\vec{p}_3, \lambda_h)\, M^{\mu\alpha}\, u(\vec{p}_1, \lambda_p)\, \xi_\alpha(\lambda_d)$ are evaluated in the system with the OZ axis along the photon momentum. In obtaining these expressions gauge invariance has been used to eliminate the time component of the current.

Integration of Eq. (14) over the lepton angles leads to the expression

$$\frac{d\,\sigma\,(e^+e^-)}{d\,\Omega_\gamma d\,m_\gamma} = \frac{\alpha^2 m_1 m_3 q_c \beta(1-\frac{1}{3}\beta^2)}{4\pi^2 m_\gamma p_c s}\,[\,W_T(s, m_\gamma, \theta_\gamma) + W_L(s, m_\gamma, \theta_\gamma)\,]\,, \tag{16}$$

where the interference RFs have dropped out.

An interesting observable is the ratio of the e^+e^- cross section (integrated over the allowed photon invariant masses) to the real photon cross section calculated at the same incoming energy and scattering angle. This quantity is called the conversion factor, and as a ratio it is believed to be less sensitive to many aspects of the reaction mechanism. We can cast this ratio in the form $R(s, \theta_\gamma) = R_T(s, \theta_\gamma) + R_L(s, \theta_\gamma)$, where the transverse or longitudinal conversion factor is given by

$$R_{T,L}(s, \theta_\gamma) = \frac{\alpha}{\pi q_c'\, W_T(s, 0, \theta_\gamma)} \int_{2m_e}^{m_\gamma^{max}} \beta(1-\frac{1}{3}\beta^2) q_c W_{T,L}(s, m_\gamma, \theta_\gamma)\, \frac{d\,m_\gamma}{m_\gamma}\,. \tag{17}$$

Here $q_c = \{[s-(m_3+m_\gamma)^2][s-(m_3-m_\gamma)^2]\}^{1/2}/2\sqrt{s}\,,\ \ q_c' = q_c\,|_{m_\gamma=0}$ stands for the real photon c.m. momentum and $m_\gamma^{max} = \sqrt{s} - m_3$.

IV. RESULTS OF CALCULATIONS AND DISCUSSION

The model is first tested for the real photon reaction. Fig. 2 (upper panel) shows cross sections for the reaction γ^3He→pd at $E_{\gamma_{LAB}} = 245$ MeV, related to the capture process at $T_{p_{LAB}} = 358$ MeV via time reversal. Note the unsatisfactory discrepancy between the disintegration and capture reaction measurements, known for a long time and recently pointed out again in Ref. [20]. As seen from the figure the agreement with the photodisintegration data [17,18] is quite reasonable and considerably better than with the data [19] for the capture reaction. The cross section here is determined mainly by the D component of the WF and differences between models 'a' (WF from [6]) and 'b' ([3]) show up mainly at $\theta < 90°$.

To study the importance of the different contributions to the amplitude we plot in Fig. 2 (lower panel) the energy dependence of the γ^3He→pd cross section at fixed angle. The figure shows in particular the large contribution of the internal amplitude (marked 'int' in Fig. 2). Also note that the cross section is a result of interference between all contribution, though the effect of the $^1S_0$ is relatively small. All calculations were performed in the Coulomb gauge (of course only the amplitude including the internal contribution is independent of the photon gauge). The full calculation (solid line) deviates from the data at E_γ between 100 and 300 MeV, though the disagreement is not too large. We do not show results for model 'b'. In general, it gives higher (up to 40%) cross sections at small energies, while above 50 MeV the situation is reversed.

We now discuss the e^+e^- production in pd capture and present calculations at the proton lab energy 190 MeV (corresponding to the kinematics at KVI, Groningen). The invariant mass and angular dependences of the response functions are shown in Fig. 3. The choice of

a forward angle in Fig. 3 (left panel) was made because in these conditions the longitudinal response is enhanced. Both W_L and W_{LT} are comparable in magnitude to W_T. Fig. 3 shows the sensitivity of the RFs to such ingredients of the model as the time-like FFs, the "negative energy" components G_-, H_- in the pd^{3}He vertex, and the $^1S_0$ contribution. The contribution of the components G_-, H_- is small, which can be explained by a cancellation between M_{int} and the terms in M_{ext} proportional to γ^μ. Backward angles are less favourable for studying the longitudinal response, which is almost always heavily suppresed compared to W_T. The exception is at large m_γ, close to the kinematical limit. For that reason we do not present the m_γ dependence for backward angles.

Fig. 3 (right panel) demonstrates the angular dependence at fixed m_γ= 65 MeV (which is about $\frac{1}{2}m_\gamma^{max}$). The transverse RF has a dependence similar to that for the real photons. The longitudinal RF is quite large at forward angles and diminishes at backward angles. The interference RFs W_{TT} and W_{LT} also show up in the forward hemisphere. The interference RFs vanish at $\theta_\gamma = 0^\circ$ and 180° because of the rotational symmetry around the photon momentum in this kinematics.

From the experimental point of view the cross section integrated over the photon invariant masses and the conversion factor are of considerable interest. These observables are plotted on Fig. 4.

Results for $R(s, \theta_\gamma)$ (Fig. 4 , lower left panel) are almost independent of the model for the WF, despite differences between the cross sections for these WFs (Fig. 4 , upper left panel). The effect of the em FFs also turns out to be very small in this kinematics, of the order of 1%. In general the longitudinal response is more sensitive to the FFs (see also Fig.2); however, after integration over m_γ the longitudinal cross section becomes extremely small compared to the transverse one (Fig. 4, upper left panel) except at very forward angles. This makes the study of the longitudinal response in this integrated observable experimentally difficult. On Fig. 4 we also show a model independent estimate for the conversion factor, which follows from Eq. (17) by neglecting $W_L(s, m_\gamma, \theta_\gamma)$ and the invariant mass dependence of the transverse response, i.e., assuming that $W_T(s, m_\gamma, \theta_\gamma) \approx W_T(s, 0, \theta_\gamma)$. On average, the deviation between the $R(s, \theta_\gamma)$ in our model and the above estimate are of the order of 5%.

At higher energy $T_p = 350$ MeV ($m_\gamma^{max} = 229.8$ MeV) one expects a larger influence of the FFs. The differences between the ^{3}He models 'a' and 'b' in the conversion factor are negligible and only calculations with the model 'a' are presented. As it is seen, the FFs modify primarily the longitudinal cross section, because the transverse one gets its main contribution from the low m_γ region, where q^2 dependence of the FFs can be neglected. Compared to $T_p = 190$ MeV, the weight of the longitudinal cross section is now enhanced and as a result the conversion factor is more sensitive to the FFs, though the effect is still not larger than 5-7%.

Note, that the time-like FFS of the deuteron and ^{3}He, when extrapolated from $q^2 < 0$ region, rapidly increase with increasing q^2. At $\sqrt{q^2} = 230$ MeV, for example, they are increased by a factor two compared to their values at q^2=0. This may not be quite realistic, since the extrapolation does not take into account the off-shell effects in the em vertices and propagators. The general problem of the (half off-shell) time-like form factors for a weakly bound composite system like the deuteron or ^{3}He is interesting, and will be addressed in future work.

In conclusion, a covariant and gauge invariant approach has been developed for the p+d

$\leftrightarrow$ ^{3}He+γ^* reactions. The agreement with data for the ^{3}He photodisintegration is reasonable, indicating that the approach seems to account for the basic mechanisms of this process over a wide range of energies. An important element of the approach is the internal amplitude needed to ensure gauge invariance. The contribution of this part of the amplitude is sizeable, which goes in line with the observations made in Ref. [24].

A mechanism which is missing in this approach is the initial- (or final-) state pd rescattering, although part of it is effectively taken into account by the ^{3}He diagram and the internal contribution. The effects of explicitly including the pd interaction will be studied in a forthcoming publication [25]. Predictions have been made for the dilepton production experiments under way in Uppsala (TSL) and Groningen (KVI). In general, the longitudinal W_L and the interference W_{LT} response functions are more sensitive to the time-like form factors. However, this effect can only be seen at forward angles where W_L and W_{LT} are comparable in magnitude to W_T, or at large angles and high photon invariant masses close to the kinematical limit. Finally, we have calculated the conversion factor, which proves to be an almost model-independent observable.

ACKNOWLEDGMENTS

We thank Robert Wiringa for calculating the ^{3}He-d and ^{3}He-d* overlap integrals. We would also like to thank Justus Koch, Ulla Tengblad, Jan Ryckebusch and Rob Timmermans for useful discussions, and Betsy Beise for sending data file with the deuteron form factors. This work is supported by the Fund for Scientific Research-Flanders (FWO-Vlaanderen).

REFERENCES

[1] E. Traneus, T.B. Bright, B. Höistad, R. Johansson, J. Thun and G.S. Adams, Nucl. Phys. **A613** (1997) 267

[2] N. Kalantar-Nayestanaki, Nucl. Phys. **A631** (1998) 242c

[3] G. Fäldt and L.-G. Larsson, J.Phys. G: Nucl. Part. Phys. **19** (1993) 171.

[4] R. Schiavilla, V. R. Pandharipande and R. Wiringa, Nucl. Phys. **A 449** (1986) 219.

[5] R. B. Wiringa, V. G. J. Stoks and R. Schiavilla, Phys. Rev. **C 51** (1995) 38.

[6] J.L. Forest, V.R. Pandharipande, S.C. Pieper, R.B. Wiringa, R. Schiavilla and A. Arriaga, Phys. Rev. **C 54** (1996) 646; http:/www.phy.anl.gov/theory/research/overlap/

[7] F. E. Low, Phys. Rev. **110** (1958) 974.

[8] B. Sakita, Phys. Rev. **127** (1962) 1800.

[9] J. Govaerts, J.L.Lucio, A. Martinez and J. Pestieau, Nucl. Phys. **A 368** (1981) 409.

[10] D. Van Neck, A. E. L. Dieperink and O. Scholten, Nucl. Phys. **A 574** (1994) 643.

[11] F. Gross and D. O. Riska, Phys. Rev. **C 36** (1987) 1928.

[12] R. Arnold, C. E. Carlson and F. Gross, Phys. Rev. **C 21** (1980) 1427

[13] W. W. Buck and F. Gross, Phys. Rev. **D 20** (1979) 2361.

[14] G. E. Brown, Mannque Rho and W. Weise, Nucl. Phys. **A 454** (1986) 669; M. Gari and W. Krumpelmann, Z. Phys.,**A 322** (1985) 689; R. Williams, S. Krewald and K. Linen, Phys. Rev. **C 51** (1995) 566.

[15] J. S. McCarthy, I. Sick and R. R. Whitney, Phys. Rev. **C 15** (1977) 1396.

[16] A. Yu. Korchin and O. Scholten, Nucl. Phys. **A 581** (1995) 493.

[17] H. J. Gassen et al., Z. Phys. **A 303** (1981) 35 .

[18] P. E. Argand et al., Nucl. Phys. **A 237** (1975) 447.

[19] J. M. Cameron et al., Nucl. Phys. **A 424** (1984) 549.

[20] N. R. Kolb et al., Phys. Rev. **C 49** (1994) 2586.

[21] N. M. O'Fallon et al., Phys. Rev. **C 5** (1972) 1926.

[22] C. C. Chang et al., Phys. Rev. **C 9** (1974) 1300.

[23] J. R. Stewart et al., Phys. Rev. **138** (1965) B372.

[24] S. I. Nagorny, Yu. A. Kasatkin and V. A. Zolenko, Phys. Lett. **B 316** (1993) 231.

[25] A. Yu. Korchin et al., in preparation.

FIGURES

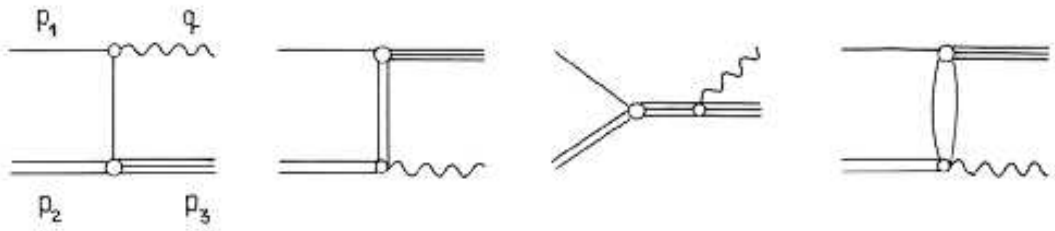

FIG. 1. Diagrams corresponding to the external amplitude.

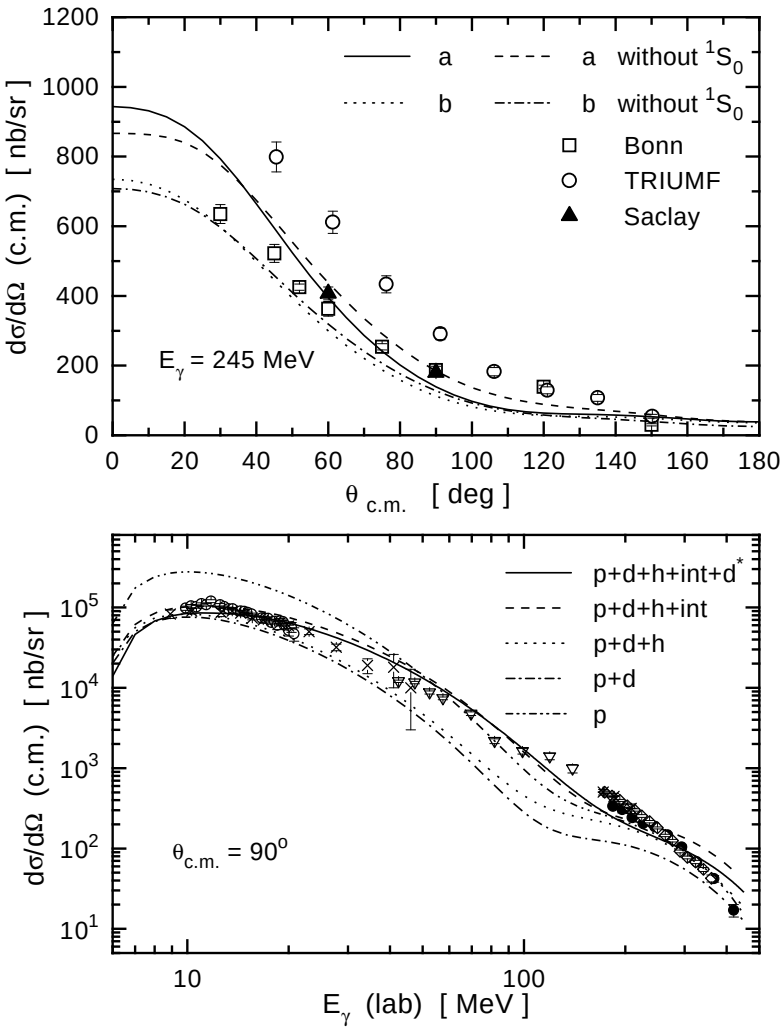

FIG. 2. Cross section for the γ^3He $\rightarrow$ pd reaction. Upper panel: angular distribution, lower panel: energy dependence. Curves on the upper panel are: solid and dashed ones for the model 'a' (WF from [6]), dotted and dash-dotted ones for the model 'b' (WF from [3]). Dashed and dash-dotted lines are calculations without $^1S_0$ amplitude Eq. (11), solid and dotted lines include all contributions. The photodisintegration data are taken from [17] and [18]. The TRIUMF points are calculated from the capture data [19] at $T_p = 350$ MeV. Calculations shown on the lower panel are performed with model 'a'. The different curves correspond to calculations including different contributions to the reaction amplitude. Data are from : $\diamond$ [18], $\bigtriangledown$ [21], $\bullet$ [17], $\circ$ [22], $\times$ [23], and $*$ [20].

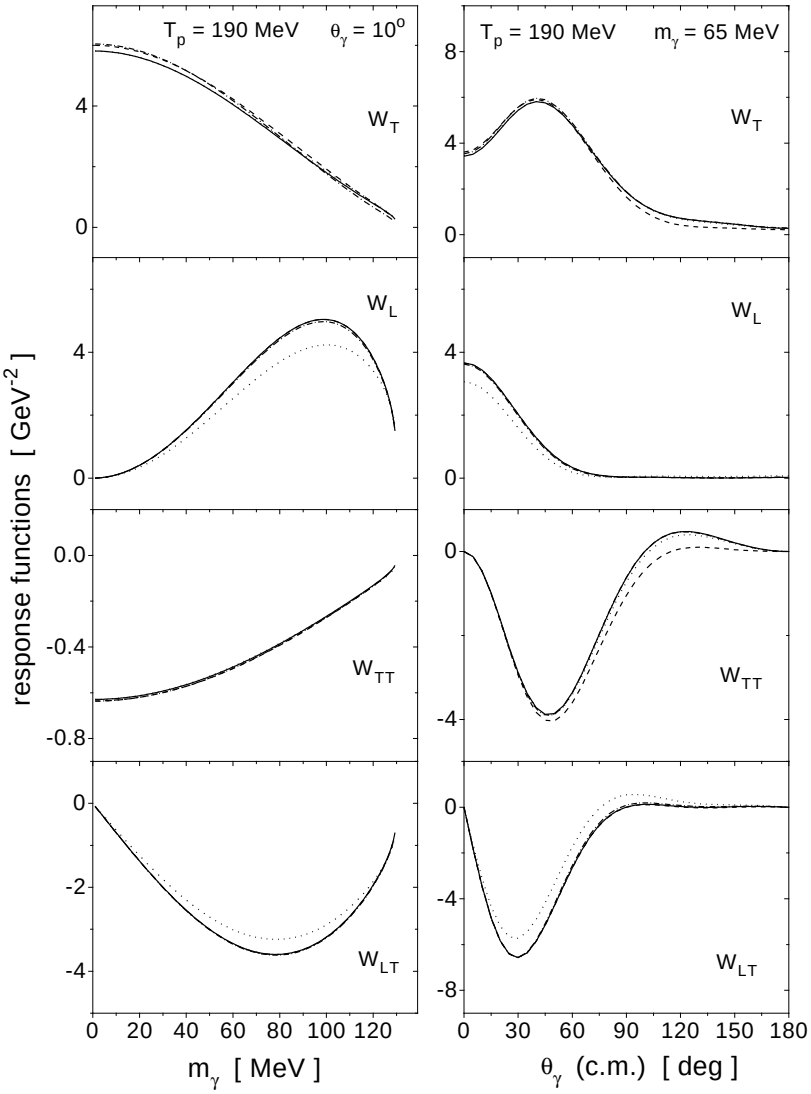

FIG. 3. Response functions for the e^+e^- production in pd capture for proton LAB energy 190 MeV. Left panel: photon invariant mass distribution at $\theta_\gamma = 10^\circ$, right panel: angular distribution at fixed m_γ=65 MeV. Calculations are performed in the model 'a'. Solid lines are the full calculations, dashed ones are obtained without the $^1S_0$ contribution. Dotted lines are the results when the em FFs are switched off, dash-dotted lines are results without the G_-, H_- components in the pd^{3}He vertex.

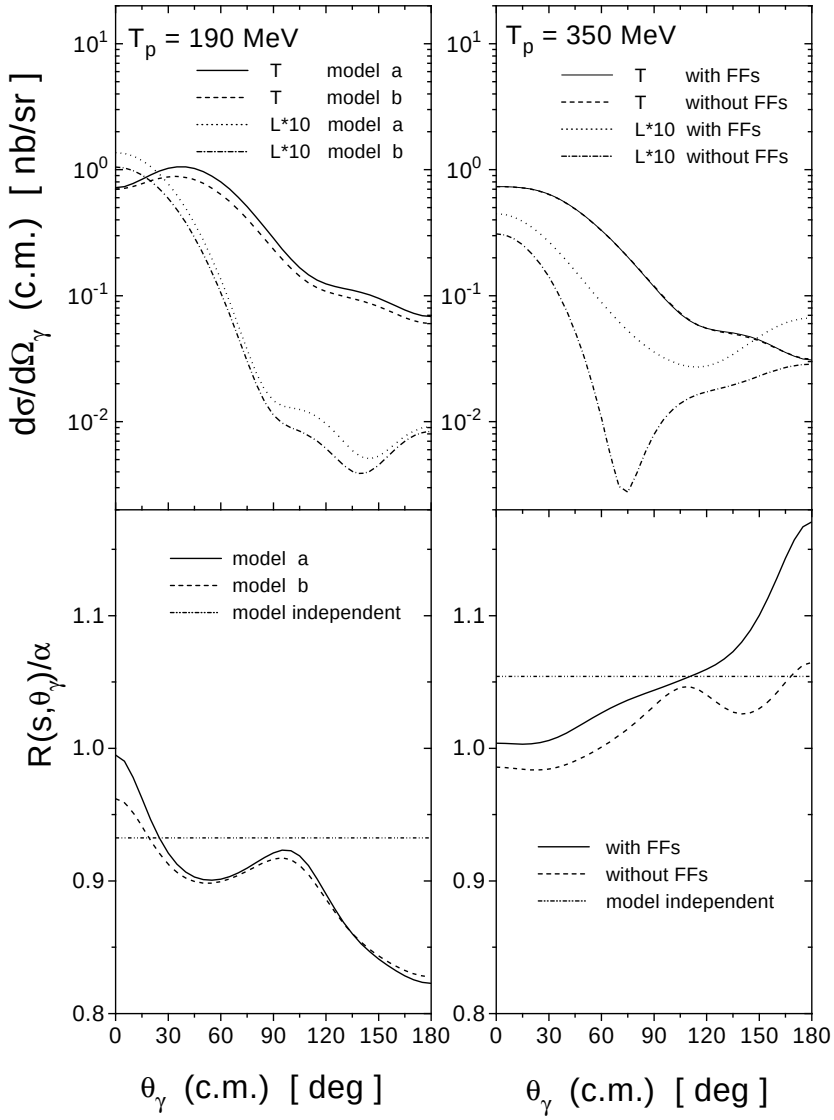

FIG. 4. Angular dependence of the cross section integrated over m_γ (upper panel) and the conversion factor devided by the fine-structure constant (lower panel). On the left panels the transverse (T) and longitudinal (L) cross sections are calculated with different models for ^{3}He WF. The right panels show the effect of the form factors. The model independent estimate for the conversion factor (see text) is shown by the dash-double-dotted lines.